Maritime Technology and Research

https://so04.tci-thaijo.org/index.php/MTR

Research Article

Motion and structural analyses of a drillship under hurricane conditions and ice impact loading

Muthu Selvakumar Nagarajan[1,*], Srinivasan Chandrasekaran[1,2,3,4], Rajiv Sharma[1], Ermina Begovic[5], Sirirat Jungrungruengtaworn[3] and Nonthipat Thaweewat[3]

[1]*Department of Ocean Engineering, Indian Institute of Technology Madras, Chennai, India*
[2]*Department of Structural Engineering, University of Federico II, Naples 80125, Italy,*
[3]*Department of Maritime Engineering, Faculty of International Maritime Studies, Kasetsart University, Sriracha campus, Chonburi 20230, Thailand*
[4]*International College, Kasetsart University, Bangkok 10900, Thailand*
[5]*Department of Industrial Engineering, University of Naples Federico II, Naples 80125, Italy*

[*]*Corresponding author's e-mail address: oe20d012@smail.iitm.ac.in*

Article information
Received: October 1, 2024
Revision: January 30, 2025
Accepted: February 5, 2025

Keywords
Drillship;
Environmental loads;
Motion response analysis;
Free-float test;
Hydrodynamic forces;
Hurricane sea states;
Ice impact

Abstract

The goal of the study is to understand drillship structural behavior under extremely hazardous hurricane conditions, as well as the variables influencing their strength and stability. In the present study, two cases are considered: a drillship is analyzed under sea states of severe storm conditions using hurricane data from the Gulf of Mexico, and ice loads acting as impact loads. Studies show that the drillship experienced instability caused by the excessive roll and pitch response motion. The critical design shear stress and longitudinal bending moment are predominantly affected by the amplified pitch response in the moonpool. The results illustrate details of the motions induced by environmental loads, free float tests, a combination of hydrodynamic diffraction and Froude- Krylov forces, impact analysis, and RAO-based time and frequency domain studies. These are very useful insights for the design of drillships under impact loads.

Nomenclature

Abbreviations

CB	Centre of Buoyancy (m)
CF	Centre of Flotation (m)
CG	Centre of Gravity (m)
DOF	Degree of Freedom
DWT	Deadweight (kg)
GoM	Gulf of Mexico
IMO	International Maritime Organization
ITTC	International Towing Tank Conference
JONSWAP	Joint North Sea Wave Project Spectrum
LCG	Longitudinal Center of Gravity (m)
PSD	Power Spectral Density (m^2 s (or) deg^2 s)
RAO	Response Amplitude Operator (m m^{-1} (or) deg m^{-1})

RMS	Root Mean Square
SD	Standard Deviation
SF	Shear Force (N m^{-1})
TCG	Transverse Centre of Gravity (m)
VCG	Vertical Centre of Gravity (m)

Annotations

A_{wp}	Area of Waterplane (m^2)
A_{wetted}	Area of Wet Surfaces (m^2)
b_m	Moonpool Breadth (m)
B	Molded Drillship Overall Breadth (m)
$B_{waterline}$	Waterline Maximum Beam (m)
C_B	Block Coefficient
C_{ij}	Hydrodynamic Damping Coefficient Matrix (kg s^{-1})
D	Overall Water Depth (m)
D_i	Ice Cone Depth (m)
D_0	Current Depth at Zero Speed (m)
f	Frequency (rad s^{-1})
f_{drag}	Multiplying Factor for Drag
f_{slam}	Multiplying Factor for Slam
F	Drillship Freeboard (m)
$F_{ij}(t)$	Excitation Forces (N)
$\overline{F_0}$	Force Amplitude (N)
g	Acceleration-Induced Gravity (m s^{-2})
h	Ice Thickness (m)
H_S	Significant Wave Amplitude (m)
I_{axis}	Mass Moment of Inertia for Rotational DOF (kg m^2)
k_{axis}	Radius of Gyration about Coordinate Axes (m)
K_{ij}	Hydrodynamic Stiffness Coefficient Matrix (kg m^{-1})
l_m	Moonpool Length (m)
L_b	Ice-Breaking Length (m)
L_C	Characteristic Length of Ice (m)
L_{OA}	Overall Length (m)
$L_{waterline}$	Length of Waterline (m)
L_{PP}	Length Between Perpendiculars (m)
$[M_a]$	Added Mass Matrix (kg)
M_{ij}	Hydrodynamic Added Mass Coefficient Matrix (kg)
M_{ij}(t)	Excitation Moments (Nm)
P	Pressure (pa)
$R_{direction}$	Force Coefficient of Wind (Ns^2m^{-2})
s_u^+	Spectral Density of Wind
T	Drillship Draught (m)
T_z	Period of Zero Crossing (s)
T	Time Period (s)
$\bar{T}$	Period of Ice (s)
U_0	Current Surface Velocity (m s^{-1})

$\overline{U}$	Mid-Profile Current Speed (m s^{-1})
$\overline{U}_{10}$	1-Hr Mean Wind Speed at Altitude of 10 m Above MSL (m s^{-1})
V	Velocity Along Body Plane Surface (m s^{-1})
w(x)	Distribution of Weight Across Drillship (kN)
X	Structure Displacement (m)
$\dot{X}$	Structure Velocity (m s^{-1})
$\ddot{X}$	Structure Acceleration (m s^{-2})

Greek symbols

α	Angles of Cutout (deg)
$\bar{\alpha}$	Phillips Constant
ρ_{air}	Air Density at Sea Level (kg m^{-3})
ρ_w	Ocean Saline Water Density (kg m^{-3})
Δ_{weight}	Displacement of Weight (mt)
∇_{volume}	Displacement of Volume (m^3)
$\Delta(x)$	Displacement due to Drillship Deep Draught (ton)
ω	Natural Frequency (rad s^{-1})
ω_p	Peak Frequency (rad s^{-1})
σ_f	Ice Crushing Strength (MPa)
γ	Peakedness Parameter
γ_{steel}	Weight Per Unit of Steel (kg m^{-3})
ϕ	Velocity Potential Function (m^2 s^{-1})
ζ	Free Surface Elevation (m)

1. Introduction

The epicentres of oil and gas drilling are shifting to the Arctic and sub-Arctic regions, imposing more harsh and challenging environmental conditions. Operating drillships in ice-covered waters impose higher risks and unique challenges to structural stability and operational safety. The Offshore sector is compelled to supplement the growing energy demands through exploration and production activities in Arctic regions. Drillships outfitted with drilling rigs, derricks, and advanced machinery are the most suitable candidates (American Bureau of Shipping. 2011; DNV-RP-F205, 2010; Chandrasekaran et al., 2023; Srinivasan & Nagavinothini, 2019; Chandrasekaran & Selvakumar, 2023). Prior to deploying drillships in these regions, challenges arising from snow and iceberg loads draw attention. The ship-shaped hull form facilitates easy maneuvering in overall water profundities of up to 3500 m (Norwood & Dow, 2013; Chandrasekaran & Jain, 2016; Mauro et al., 2023; Rawson & Tupper, 2011). The additional internal storage and versatile load capabilities of new-generation drillships enable them to function in hostile conditions (American Petroleum Institute. 2007; Srinivasan et al., 2022; Korde, 1998); for example, the Mobile offshore drilling units (MODU) with compatible hull forms of enhanced storage enabling drilling operations in isolated regions (Lee & Roh, 2018; Sharma, et al., 23010; You et al., 2008). Since innovative hull forms have long-term influence on the structural design of drillships, the focus is to examine the dynamic response under impact loads caused by ice (DNV, 2011, 2021; Yuda et al., 2015; do Vale Machado & Fernandes, 2022). **Figure 1** shows a typical drillship, geometric details, and major components. Apart from the core components, namely rig floor, berthing facilities, derrick, crown block, engine room, moonpool, cranes, dynamic position thrusters, heave compensator, living quarters, riser stacks, helideck, and pipe racks, the exploration unit's moonpool aperture and cantilever extension are positioned beneath the derrick, over through the drillship, and down to the ship hull. The drilling activities provide unique challenges because of their geometric positioning and operation loads, in combination with the critical

environmental loads that arise in deepwater zones (Chandrasekaran & Purushotham, 2024; Olapoju, 2023; Suja & Chandrasekaran, 2024). The integration of environmental performance assessment in ports and ultra-deepwater structures is crucial. This integration can improve regulatory compliance, minimize environmental impacts, and promote better sustainability practices (Saengsupavanich et al., 2009). To ensure these vessels' safe and efficient functioning, it is crucial to comprehend their responses to impact loads induced by ice.

The new generation drillships are expanding away from the continental shelf to reach deeper water depths. Their capabilities to possess high velocity (about 12 - 16 knots) with self-propulsion and operate in remote areas under rough weather can be examined only through a very precise estimation of the drillship platform hull's response motion (Yang et al., 2016; Yu et al., 2019; Tikhonov & Komissarenko, 1991). This is imperative as, due to harsh storm conditions, a drillship capsized at the oil and gas reserves located in deep Seacrest (Choi et al., 2011; IMO, 2008; ITTC, 2021; Molin, 2001; Chandrasekaran, 2020; Liu et al., 2022). As their hydrodynamic response under severe sea states becomes vital, the present research examines a drillship's response to ice impact loads in addition to loads arising from hurricane sea states. The primary objective is the examination of structural responses of a drillship consisting of a rectangular moonpool aperture in a deeper pelagic zone (at 3,200 m water depth). The moonpool aperture is expanded at the Waterplane Area (WPA) in the center, to provide a heave natural frequency. This is narrowed towards the keel portion to improve the drillship vessel's storage capability and efficiency. Its dynamic responses to hurricane sea states with various return periods of 10, 100, 1,000, and 10,000 years (referred to as low, moderate, high, and very high sea states) are examined at ultra-deepwater under tropical storm conditions.

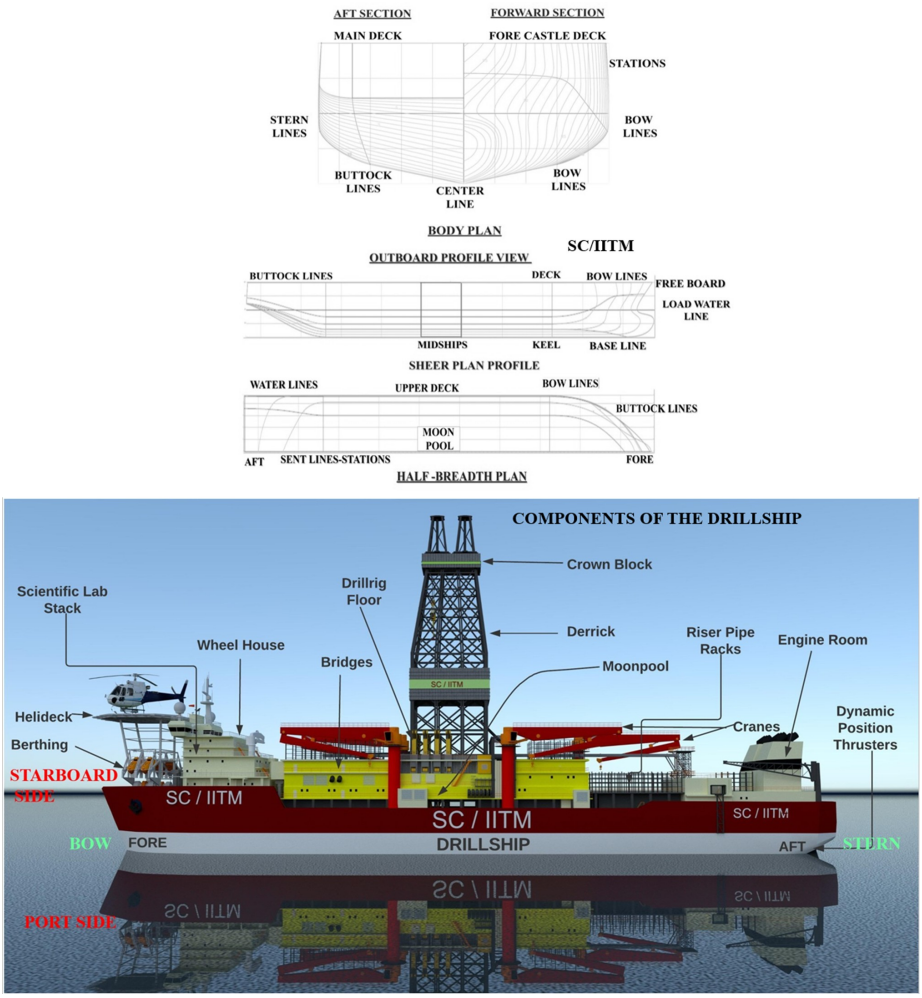

Figure 1 Geometry (top) and side view (bottom) of considered drillship.

The numerical model accounts for the deepwater seabed, the geology of the area, and its operational depth. For the impact analysis, ice thickness, crushing strength, the velocity of icebergs, wave amplitude, wind speed, and current velocity are considered. A preliminary design, in accordance with IMO and ABS regulations (DNV-RP-F205, 2010; IMO, 2008; ITTC, 2021), is carried out under environmental loads such as waves, wind, and current.

Table 1 Structure-specific features of drillship.

Architectural Features	Symbol	Magnitude	Unit
Length Overall	L_{OA}	242.1	m
Length Between Perpendiculars	L_{PP}	228	m
Beam Molded Breadth	B	42	m
Scantling Draught Molded Depth	T	19.6	m
Moonpool Length	l_m	25	m
Moonpool Breadth	b_m	18	m
Moonpool Position (Through Transom)	P	101.732	m
Cutout Slant Angle	α	90	deg
Operating and Survival Draught (Deep Draught) at MWL	T_{deep}	12	m
Transit Draught (Light Draught) at MWL	T_{light}	10	m
Free Board	F	7.2	m
Variable Deck (Operating and Transit)		20,535	mt
Transit Speed	$v_{transit}$	12.5	kn

The critical structural response and resistance properties are numerically evaluated. The hydrodynamic analysis of the responses carried out under ice impact, current, wave drift, and wind are reported. The analysis of the critical shear force and the computed design longitudinal bending moment are investigated in the frequency domain. Drillships are large maritime vessels mainly designed for deep-water drilling for oil and gas exploration. It is a modified version of an ordinary seagoing monohull ship with substructures, including cantilevers and a moonpool for drilling platforms. The hull is built to accommodate the amidships drilling equipment, which is positioned in the centre of the deck. Due to their high loading capacity and versatility, dynamically positioned self-propelled drilling vessels are often increasingly employed for offshore drilling. The novelty of this study is to analyze the dynamic responses of a drillship to an ice impact using numerical modeling. It thoroughly examines the drillship's responses to various ice-induced forces by considering variables including ice thickness, ice velocity, and crushing strength. This aids in the optimization of design parameters for increased efficiency and safety. In the process of designing drillships, this research confidently proposes potential design improvements to minimize negative performance impact while ensuring safety is maintained (Kaewkhiaw, 2025). The literature has not covered the features of the drillship hydrodynamic response in severe sea conditions, and the investigation of the environmental impact of drillship operations in ice-covered regions is scarce in the literature.

2. Methodology

This methodological approach employed in this research study involves a comprehensive analysis of the dynamic behavior of a drillship under the influence of ice impact. The model for the ultra-deep ocean is developed using the measurements of a generic hull shape with a rectangular moonpool from CAD software. The total length and molded breadth are (242.1, 42 m) for a dead weight of 3,98,561 kN. The total weight includes the weight of the drilling derrick, deck supplies, production machinery, and other topside components. As seen in the body plan view, the hull form is center-plane symmetric. A transom-shaped stern is considered for designing the hull form. **Table 1** lists the geometrical properties, and **Table 2** summarizes the hydrostatic characteristics of the drillship considered in the analyses.

Table 2 Hydrostatic properties.

Hydrostatics Properties	Symbol	Magnitude	Unit
Centre of Buoyancy	CB	121.481, -0.428, -2.280	m
Centre of Floatation	CF	115.453, -0.418,0	m
Weight Displacement	Δ_{weight}	1,05,657	mt
Volume Displacement	∇_{volume}	29,953.700	m^3
Gross Volume	V	1,31,938	m^3
Water Plane Area	A_{wp}	8,074.570	m^2
Wetted Surface Area	A_{wetted}	8,776.870	m^2
Gross Area	A	25,613.490	m^2
Waterline Length	$L_{waterline}$	223.906	m
Maximum Waterline Beam	$B_{waterline}$	41.510	m

In order to complete the initial critical design evaluations and reconciliation calculations, the software computations are complemented by manual calculations. The wave loading is simulated by the AQWA solver using the potential flow theory, which uses a predictor-corrector numerical integration technique to compute the response in real-time at each time interval. Based on AQWA solver free float tests, motions induced by environmental loads, combined hydrodynamic diffraction and Froude- Krylov forces, and RAO-based time and frequency domain studies for all 6 DOF are obtained. Following model creation, a three-dimensional panel approach is used to mesh the hull. Due to the variety of ice conditions that might occur over a drillship's service life, predicting ice loads carries a significant degree of risk. These are categorized as broken ice, level ice, icebergs, and ice ridges. Under ice stresses, floating bodies exhibit several forms of failure, including creep, spalling, cracking, buckling, and crushing. Both in location and time, ice loads exhibit unpredictable changes. These are divided into two categories: (i) total or global loads, and (ii) localized loads or pressure. Local loads have an impact on the members at connections, whereas global loads have a severe impact on the drillship platform's overall motion and stability.

3. Ship motion analysis: governing equations

Following the "strip hypothesis," members in the two-dimensional transversal slices are strongly connected. One of the basic assumptions made is that the wave amplitude is relatively small and the vessel speed is slow; this is required to reach an acceptable solution convergence while solving the governing equation. Viscous forces are ignored from consideration, and the fluid medium is presumed to be incompressible and follows Poiseuille's law; the irrotational direction of flow characterizes the fluid. When the potential velocity function calculated by Poisson's calculation is in control of the fluid medium, the following equations are valid:

$$\nabla.\nabla\phi = \frac{\partial^2\phi}{\partial x^2} + \frac{\partial^2\phi}{\partial y^2} + \frac{\partial^2\phi}{\partial z^2}; \quad (1)$$

The observed boundary conditions follow:
The condition for the ocean's bed and the state of the surface:

$$\frac{\partial\phi}{\partial\zeta} = \vec{v}.\vec{n}; \frac{\partial\phi}{\partial z} = 0, \quad z = -D; \quad (2)$$

The surface state requirements for a dynamically free surface state:

$$\frac{\partial\phi}{\partial t} = -g\zeta - \frac{1}{2}|\nabla\phi|^2, \quad z = \zeta(x,y,t) \quad (3)$$

The following conditions are reliable for the P of the body:

$$\nabla\phi \to 0 \quad x \to \infty \quad (4)$$

The hydrodynamic pressure, moments, and forces are calculated by integrating the level of pressure throughout the moistened vessel surfaces (A_{wetted}):

$$P = -\rho\left(\frac{\partial\phi}{\partial t} + \frac{1}{2}\nabla\phi.\nabla\phi + gz\right) \quad (5)$$

Excitation forces ($\vec{F}_{ij}$) and the moments (M_{ij}) acting on the surface are computed as below:

$$\vec{F}_{ij} = \iint_S P.\vec{n}\, ds \quad (6)$$

Using the pressure and force equation mentioned above, the excitation moment is derived as follows:

$$\vec{M}_{ij}(t) = \iint_S P\,(X \times \vec{n})ds \quad (7)$$

The computational potential flow solver of the Boundary Element Method (BEM) is implemented. These responses' frequency statistics, stability, and time history are evaluated using ANSYS AQWA. The convolution integration technique is applied to resolve an equation of motion:

$$[\mathrm{M_a} + \mathrm{M}]\ddot{\mathrm{X}} + [\mathrm{C}]\dot{\mathrm{X}} + [\mathrm{K}]\mathrm{X} = \vec{F}_{ij}(\mathrm{t}) \quad (8)$$

Wherein (M, K, C, M_a) stand independently for the mass, stiffness, damping, and added mass. In the frame, the emergence of a square matrix with specific dimensions $(i \times j)$, respectively. Aerodynamic loads possess an impact on drillships due to the significant derrick height in comparison to the draught. API Wind spectra (2000) are utilized to enumerate wind loads and are assumed to act in the dominant wave heading angle:

$$\frac{\omega s_u^+(\omega)}{\sigma_u(z)^2} = \frac{\left(\frac{\omega}{\omega_p}\right)}{\left[1+1.5\left(\frac{\omega}{\omega_p}\right)\right]^{5/3}} \tag{9}$$

The JONSWAP spectrum performed in the numerical analyses depicts the winter storm waves of the North Sea and is acceptable for such modest tiny fetches:

$$S^+(\omega) = \frac{\bar{\alpha} g^2}{\omega^5} \exp\left[-1.25\left(\frac{\omega}{\omega_0}\right)^{-4}\right] \gamma^{a(\omega)} \tag{10}$$

where γ is 3.3 and has an effect on the wind period besides the phases of decay and storm growth; α is taken as 0.0081. The following relationships are used to compute the shear and longitudinal bending:

$$SF(x) = \int_0^x \big(w(x) - \Delta(x)\big)dx \tag{11a}$$

$$BM(x) = \int_0^x SF(x)dx \tag{11b}$$

Deep-water currents are described as the velocity profile, which is defined as a three-point profile: the zero-speed depth (D_0), the surface speed (U_0), and the speed at mid-profile ($\overline{U}$). Ice loads, causing significant strain on the hull in polar regions, are modeled using an ice force spectrum applicable to a narrow conical structure (Chandrasekaran & Srivasatava, 2018):

$$S^+(f) = \frac{A\overline{F_0}^2 \bar{T}^{(-\delta)}}{f^\gamma} exp\left[-\frac{B}{\bar{T}^{(\alpha)} f^\beta}\right] \tag{12}$$

The variables in the equations related to ice characteristics in the Bohai Gulf region are as follows: A=10, B =5.47, and C=3.4 are constants; the L_b is generally 4 to 10 times the ice thickness, and the ice bending strength is 0.7 Mpa; Young's modulus of ice (E = 0.5 GPa); [the typical constant values are α=0.64, β=0.64, γ=3.5, δ=2.5] (Chandrasekaran & Nagavinothini, 2020).

$$\bar{T} = L_b/v; \overline{F_0} = C\sigma_f h^2 \left(\frac{D_i}{L_c}\right)^{0.34}; \text{ characteristic length of ice is, } L_c = \left[\frac{Eh^3}{12g\rho_w}\right]^{0.25} \tag{13}$$

The selected variables include ice thickness, the velocity of the ice cap, and the diameter of the ice core (Srinivasan & Nagavinothini, 2019).

4. Numerical analysis and discussions

The hull shape's imported geometry, along with the boundary conditions and modelling framework, is shown in **Figure 2**. **Tables 3 - 4** show the model's characteristics, environmental conditions, and meshing details, respectively. The optimized rectangular moonpool dimension with a 90° cutoff angle is considered (ITTC, 2021). As the location and orientation of the drilling machinery play an essential role in the dynamic response, an overall structural mass of 40,000 tons of DWT is carried and uniformly distributed throughout the hull. The study is centered on understanding how the fluid surrounding the drillship influences the forces acting on it, especially during the acceleration of hull form during critical environmental forces (Bharti et al., 2024). The motion response calculation of the drillship is based on the global reference system.

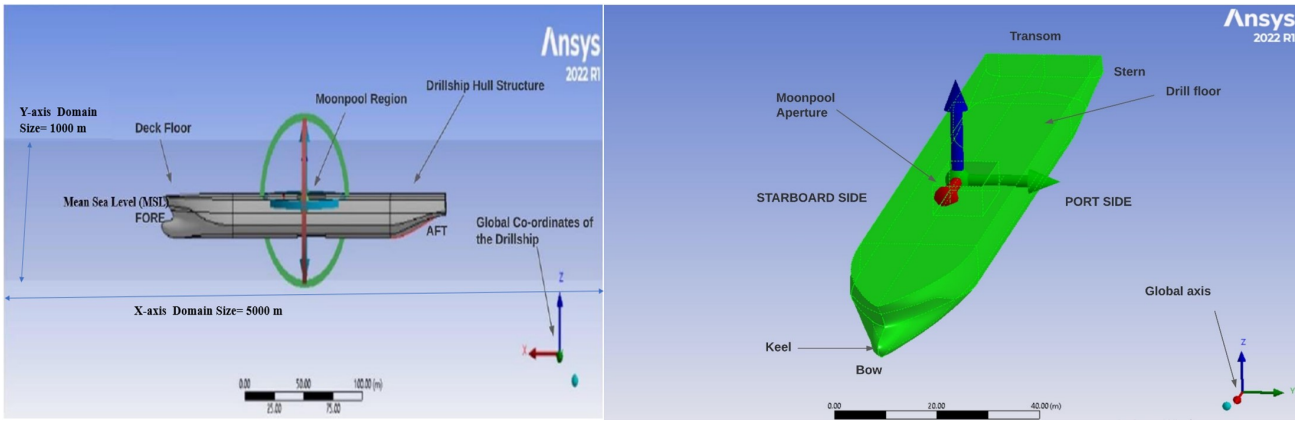

Figure 2 Boundary condition and modeling framework.

Table 3 Characteristic aspects of drillship.

Architectural Features	Symbol	Magnitude	Unit
Longitudinal CoG	LCG	97.173	m
Transversal CoG	TCG	-4.711	m
Vertical CoG	VCG	6.796	m
Gyratory Radius about Longitudinal Axis	k_{xx}	9.355	m
Gyratory Radius about Transverse Axis	k_{yy}	50.602	m
Gyratory Radius about Vertical Axis	k_{zz}	50.602	m
Rolling Mass MoI	I_{xx}	3,500,641,000	kg m^2
Pitching Mass MoI	I_{yy}	102,423,305,793.600	kg m^2
Yawing Mass MoI	I_{zz}	102,423,305,793.600	kg m^2
Other Mass MoI	I_{xy}, I_{yz}, I_{yz}	0	kg m^2
Overall Dead Weight (Self weight + payload)	DWT	40,000	ton
Air Density at Surface of Ocean Level	ρ_{air}	1.225	kg m^{-3}
Unit Weight of Steel Material	γ_{steel}	7850	kg m^{-3}
Drag Factor	f_{drag}	1	-
Slam Factor	f_{slam}	0	-
Mass Factor	f_{mass}	1	-
Wave Grid Size Factor		2	-
L_{PP}/B ratio	L_{PP}/B	5.428	-
L_{PP}/D ratio	L_{PP}/D	11.632	-
B/D ratio	B/D	2.142	-
Displacement at Deep Draught	$\Delta(x)$	1,31,938	ton
Deep Displacement/ LBD	Δ/LBD	0.662	ton m^{-3}
Block Coefficient	C_B	0.890	-

While the buoyancy forces and hull mass are estimated from the hydrostatic calculation, the longitudinal mass distribution is set as program-controlled. The boundary domains are considered significantly large (about 20 times greater than the hull size) to avoid interference effects. The vessel is assumed to operate at a forward speed of 12.5 knots.

Table 4 Environmental conditions and meshing details.

Architectural Features	Graphic Symbol	Magnitude	Unit
Overall Water Depth	D	3,200	m
Maximum Drilling Depth	$D_{drilling}$	12,192	m
Overall Storage Capacities	S	16,732	m^3
Ocean Water Density	$\rho_{sea\ water}$	1,025	kg m^{-3}
Acceleration Causing Gravity	g	9.806	m s^{-2}
Wind Force Coefficient	$R_{direction}$	1,286.250	N s^2m^{-2}
Meshing Standards			
Defeaturing Tolerance	-	0.500	m
Size of Most Significant Element	-	1	m
Peak Permitted Frequency	f	2.540	rad s^{-1}
Wave Interval	-	45	deg
Number of Intermediate Wave Directions	-	7	-
Total Number of Frequencies	-	20	-
Total Duration	-	3,000	s
Total Number of Steps	t	30,001	-
X, Y-Position for Water Surface Elevation Output	-	0	m
Domain Water Size X	-	5,000	m
Domain Water Size Y	-	1,000	m

The mesh's most significant element size is 1 m, and the analysis employs a prominence to a tolerance size of 0.5 m. The mesh analysis method uses a maximum allowed frequency (f) of 2.54 rad s^{-1}. The highest number of nodes at the surface level and maximum elements are included for the loads and motion analysis. Different mesh sizes are assessed to determine the sensitivity before the final run; for the fine mesh, the total number of surface nodes and overall elements is restricted to 60,000 units. Free float tests are considered to evaluate the hydrodynamic loads.

Figure 3 shows the RAOs in various degrees of freedom in head sea conditions for the unit wave amplitude.

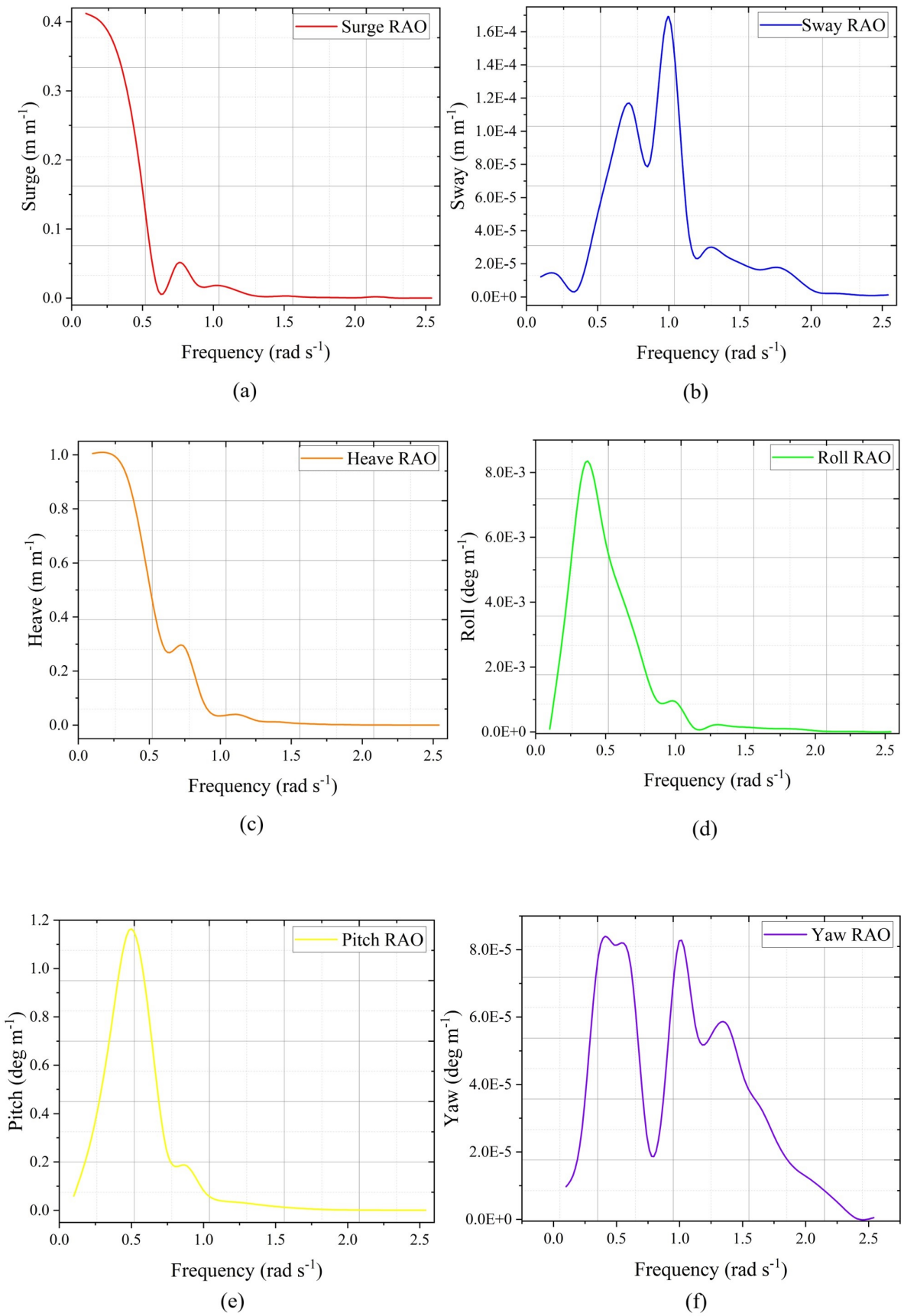

Figure 3 Response amplitudes under free float conditions; (a) RAO of Surge response, (b) RAO of Sway response, (c) RAO of Heave response, (d) RAO of Roll response, (e) RAO of Pitch response, (f) RAO of Yaw response.

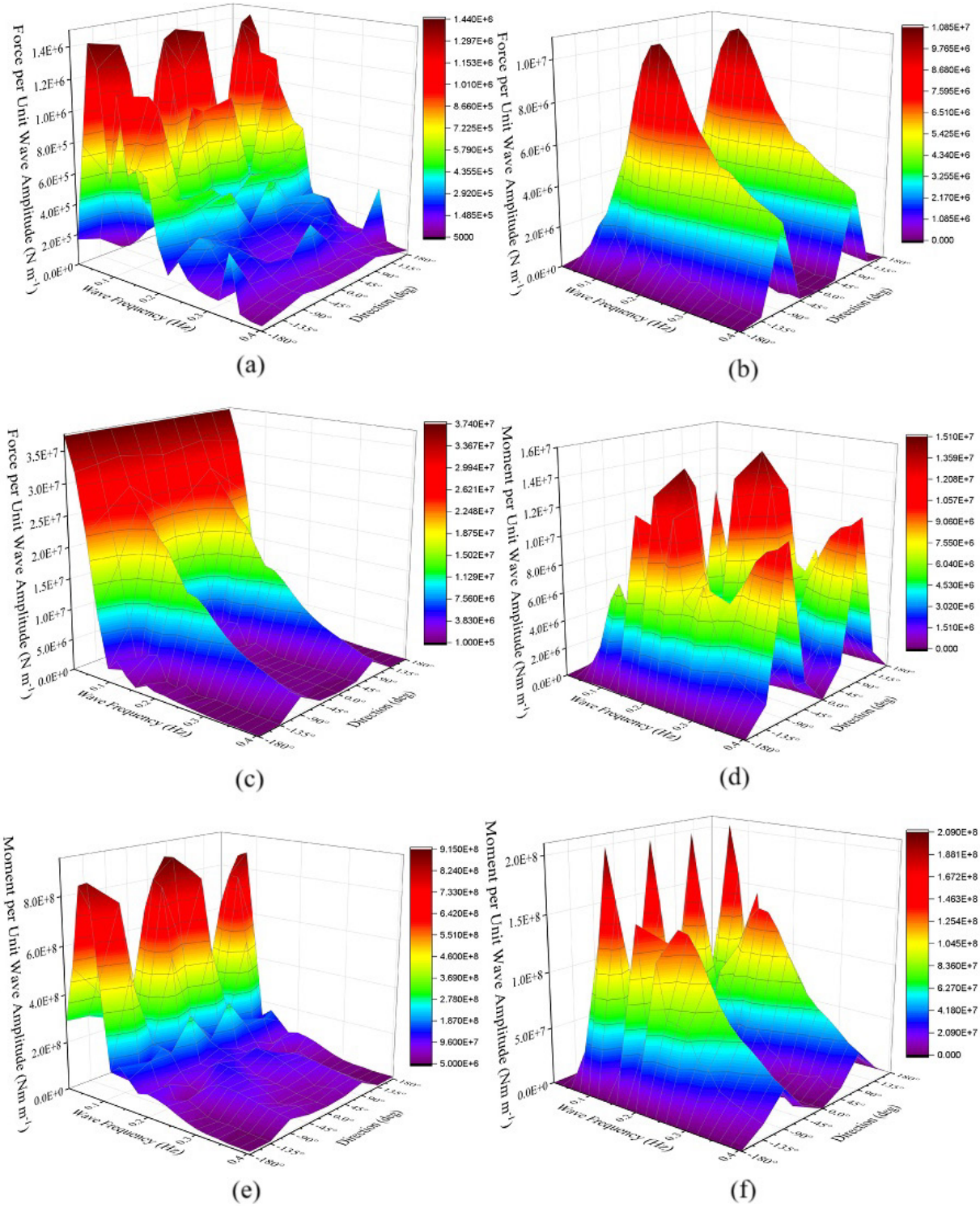

Figure 4 Wave excitation under combined diffraction and Froude-Krylov forces; (a) Surge force spectrum, (b) Sway force spectrum, (c) Heave force spectrum, (d) Roll force spectrum, (e) Pitch force spectrum, (f) Yaw force spectrum.

Figure 4 shows the force/moment spectra in different degrees of freedom under the wave excitation combination of diffraction and Froude Krylov forces.

4.1 Ice loads-impact analysis

The extreme circumstances, probable ice-structure interactions, and arctic locations provide unique challenges. The hull form is not specifically designed for operations in ice-covered regions; however, this analysis explores hypothetical scenarios in which the drillship may encounter extreme environmental conditions, including ice impacts, to evaluate the robustness and structural integrity of the design. Under ice impact stresses, floating bodies exhibit severe forms of failure. The ice loads induce transient vibration in the hull form and affect overall motion and stability. A resistance test was performed for the trimmed mesh of the drillship under a forward speed of 12.5 knots until convergence. A total resistance, as a combination of pressure and shear, is reported as 337.3 kN. The characteristics of each resistance property are displayed separately in **Table 5**.

Table 5 Resistance properties of drillship hull.

Characteristic Description	Magnitude	Units
Mesh Element Count	1.380406	million
Pressure Resistance	2,34,071.401	N
Shear Resistance	1,03,190.234	N
Total Resistance	3,37,261.636	N
Mean Pressure Resistance	1,71,490.1	N
Mean Shear Resistance	1,03,506.5	N
Mean Total Resistance	2,47,126.0	N

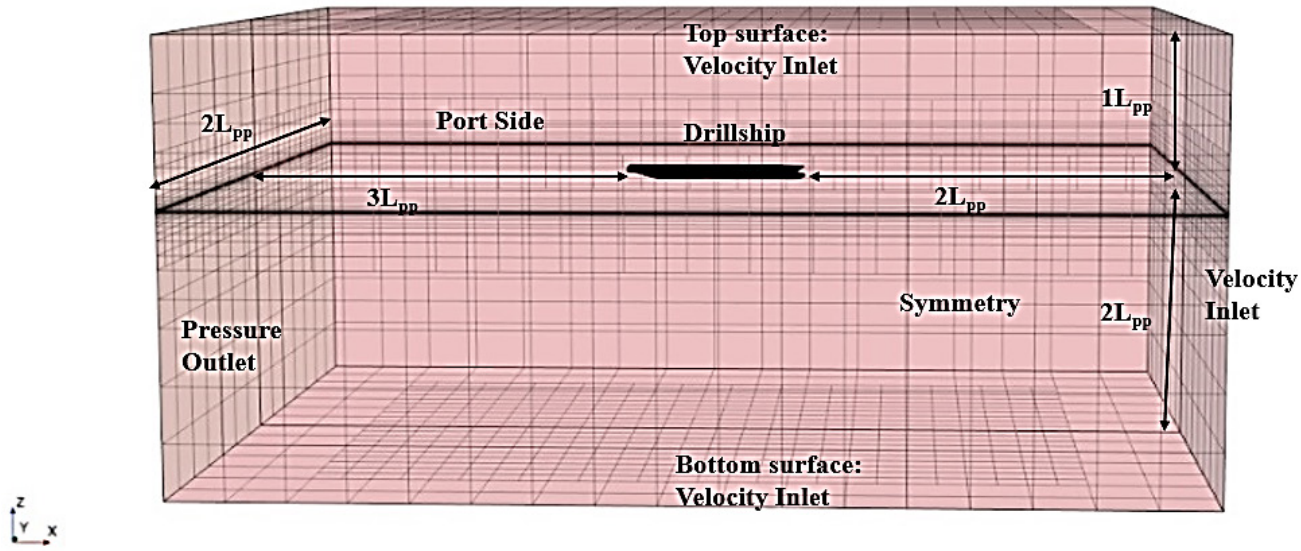

Figure 5 Boundary condition of computational domain.

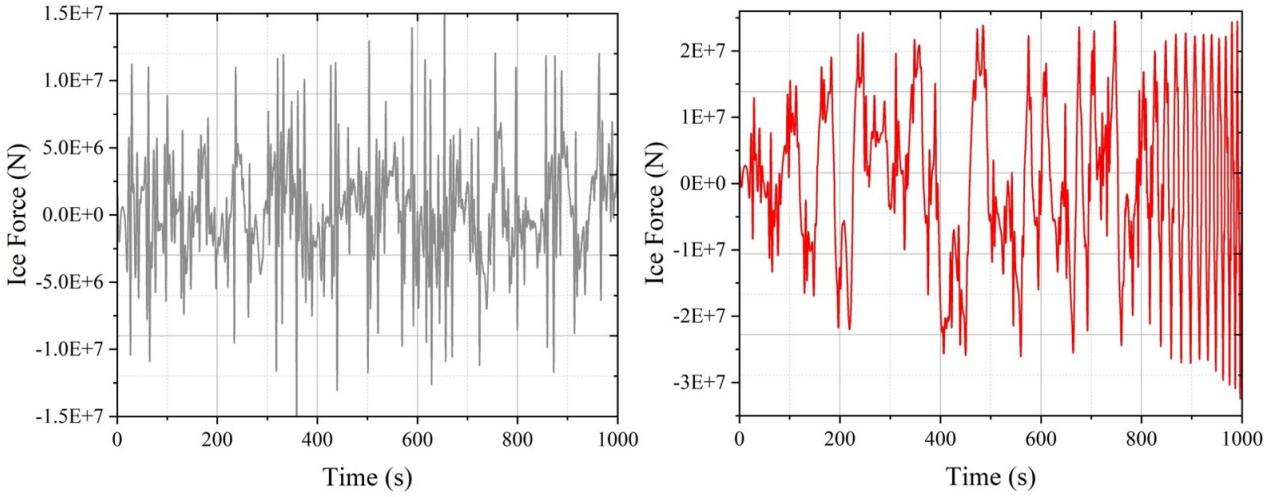

(a) (b)

Figure 6 Load time history for ice states; (a) Ice Sea state -1, (b) Ice Sea state -2.

Table 6 Ice states (Srinivasan & Nagavinothini, 2019).

Ice Sea State	Thickness of Ice h (m)	Ice Crushing Strength σ_f (MPa)	Ice Velocity (ms^{-1})	Maximum Ice Load (kN)
Ice Sea State-1	0.5	1.5	0.2	5,468.10
Ice Sea State-2	1	3	0.2	23,382.70

The time-domain response simulation has been conducted to assess the dynamic behavior of the drillship when subjected to ice impact loads. The ice impact load is inquired after to the Global X in the surge direction to the drillship's hull, considering its ice-strengthening features and the ice interaction phenomenon. Due to the sudden load after a time period of 0 sec, an impact occurs on the structural hull form.

The values provided in **Table 6** are derived based on relevance to the specific environmental conditions considered in the analysis (Srinivasan & Nagavinothini, 2019). It consists of the critical parameters of two ice states, namely Ice Sea State-1 and 2. **Figure 5** shows the boundary condition of the computational domain for the hull's resistance properties calculations. **Figure 6** shows the ice load history for the two cases, and **Figure 7** shows the shear forces/bending moments in the corresponding degrees of freedom that arise under different ice states considered in the analysis. The total surge forces are minimal when compared to all other responses. For the global load's influences, the surge and heave response in Sea State-1 phenomenally increases over time. The drillship drifts in the surge DOF with a mean shift as ice load sea states increase. The overall ice force can lead to periodic loading and induce dynamic amplification in the drillship. The sway and heave forces increase gradually over time. The total moment in the yaw response is higher, which is explicitly visible. For the ice Sea State conditions 1 and 2, pitch and yaw motions dominate the responses.

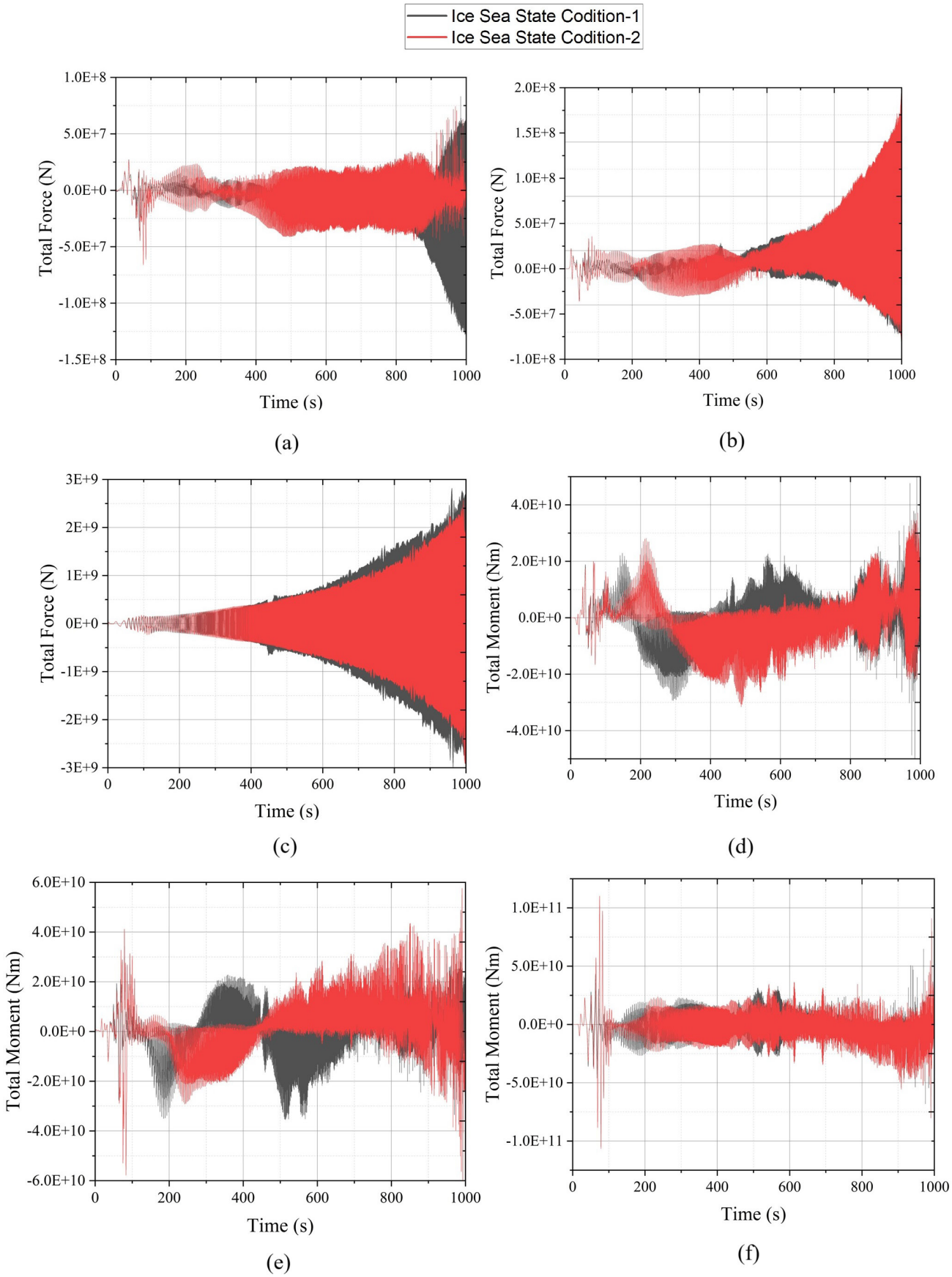

Figure 7 Force/moment under ice Sea State -1 and 2; (a) Surge, (b) Sway, (c) Heave, (d) Roll, (e) Pitch, (f) Yaw.

4.2 Hurricane environmental load cases analysis

Examining variables, including wind speed, wave height, wave duration, current velocity, and swell direction, is part of the analysis (Wang et al., 2022). The time and frequency-domain simulations are executed to study the dynamic behavior of the drillship under various sea states according to the environmental data collected for the GoM offshore region.

Table 7 Western field region of GoM: independent extreme values for hurricane winds and waves, environmental Sea State scenario (94.0 to 90.50 degrees West).

Characteristics of Sea States Description	Return period (years)	Wind Force (10 m altitude)	Waves Force (Oceanic water depth ≥ 1,000 m)		
		1-Hr mean wind speed at the height of 10 m above MSL $\bar{U}_{10}$ (m s^{-1})	Significant Wave Height H_s (m)	Zero crossing period T_z (s)	Wave Dominant Frequency (rad s^{-1})
Low	10	24.90	8.10	12.60	0.49867
Moderate	100	38.10	12.30	14.40	0.43633
High	1,000	47.60	15.40	15.80	0.39767
Very High	10,000	55.20	17.80	17.00	0.36960

Table 8 Western field region of GoM: independent extreme values for hurricane currents.

Characteristics of Sea States	Return period (years)	Current Force (Oceanic water depth ≥ 150m)			Current velocity profile	
Description		Surface speed of current U_0 (m s^{-1})	Current Speed at mid-profile $\bar{U}$(m s^{-1})	Current zero-speed depth D_0(m)	Depth (m)	Velocity (m/s)
Low	10	1.25	0.93	52.30	0	1.25
					-26.15	0.93
					-52.30	0
					-3,200	0
Moderate	100	1.91	1.43	80.00	0	1.91
					-40.00	1.43
					-80.00	0
					-3,200	0
High	1,000	2.38	1.79	100.00	0	2.38
					-50.00	1.79
					-100.00	0
					-3,200	0
Very High	10,000	2.76	2.07	115.90	0	2.76
					-57.95	2.07
					-115.90	0
					-3,200	0

The magnitudes reported in **Tables 7** and **8** are the product of site-specific knowledge. They are based on 10, 100, 1,000, and 10,000-year return periods for the GoM west area and independent extreme values for wind, waves, and current during severe storms (API 2INT-MET, 2007).

4.2.1 Hydrodynamic time response analysis- structure position vs RAO-based responses study

The hydrodynamic time response analysis is critical to analyzing the drillship's structural response in its action to cope with rapid variations in ocean currents, waves, and wind that lead to instability, especially in hostile environments. **Figure 8** depicts the drillship's response time histories and overall DOF for the four load scenarios considered for the analysis. With a time-step of 0.1s, the time-dependent hydrodynamic analysis is executed for 3,000s, capturing short-term transient responses and longer-term trends under various sea states. As can be observed, the 100-year load case experiences significant yaw and roll responses, primarily due to the coupled effects of current and wave forces. It has been demonstrated that responses across all operating levels rise with an escalation in the intensity of hurricane conditions. These combined forces have the potential to synchronize with the natural frequencies of the drilling vessel, increasing rotational movements. The yaw response, which tracks the drillship's rotation around its vertical axis, is critical, as excessive yaw can make it challenging to maintain a stable heading during operations. Likewise, roll motion, worsened by broadside waves, emphasizes the vessel's susceptibility to lateral instability under extreme loading conditions. Over a return period of 10,000 years, it is observed that the overall surge response achieves its highest level. In the time histories, it is observed that, as hurricane conditions worsen, there is a direct increase in responses across all DOFs. The pitch and surge motions become particular peaks, with the surge response, which characterizes the forward and backward motion along the vessel's longitudinal axis, reaching its highest peak during the 10,000-year return period scenario. This suggests that even dynamic positioning systems may struggle to maintain the vessel's position under such extreme conditions, potentially leading to excessive drift.

4.2.2 Hydrodynamic time response analysis- Structure Position vs PSD-based responses study

Figure 9 depicts the PSD of responses in different degrees of freedom, with the higher return period influencing the greatest spectral energy. The moderate sea state imposes a significant roll and yaw response, caused by wave and current coupled effects, while the surge motion reaches its maximum under very-high sea state circumstances. The roll motion changes based on whether the bottommost keel segment gets flooded and damaged during the bilging conditions. Under a very high sea state, the most substantial transient response is observed. Concurrent waves, wind, and current activities cause the multiple peaks observed. The vessel is balanced to remain under dynamic equilibrium, but can cause a pounding effect under large pitch and heave motion. The drillship exhibits improved motion at deep abyssal water depths for the 10-year and 100-year return periods, as seen by the reduction in the roll response peak values. It enables safe operation in the pelagic field, along with a spread-mooring mechanism to control the response up to 1,000 m of sea depth. The spectral plots in all the sea states demonstrate that the spectral energy is concentrated in a narrow band, pointing to resonant interactions between the vessel and the external forces. With the increase in the severity of hurricanes, responses in entire active degrees of freedom show a spike, reflecting the vessel's sensitivity to such extreme events. The response shows a periodic pattern and varies concerning its mean position, underscoring the importance of accurately predicting dynamic equilibrium to prevent large, destabilizing motions. Through a detailed examination of these factors, a comprehensive understanding can be developed of how environmental forces influence the motion behavior of drillships in different operational scenarios, particularly during severe weather conditions or deep water operations. This understanding is crucial for devising effective mitigation strategies, including enhancing mooring systems and hull designs, and implementing active damping mechanisms to improve vessel stability and safety.

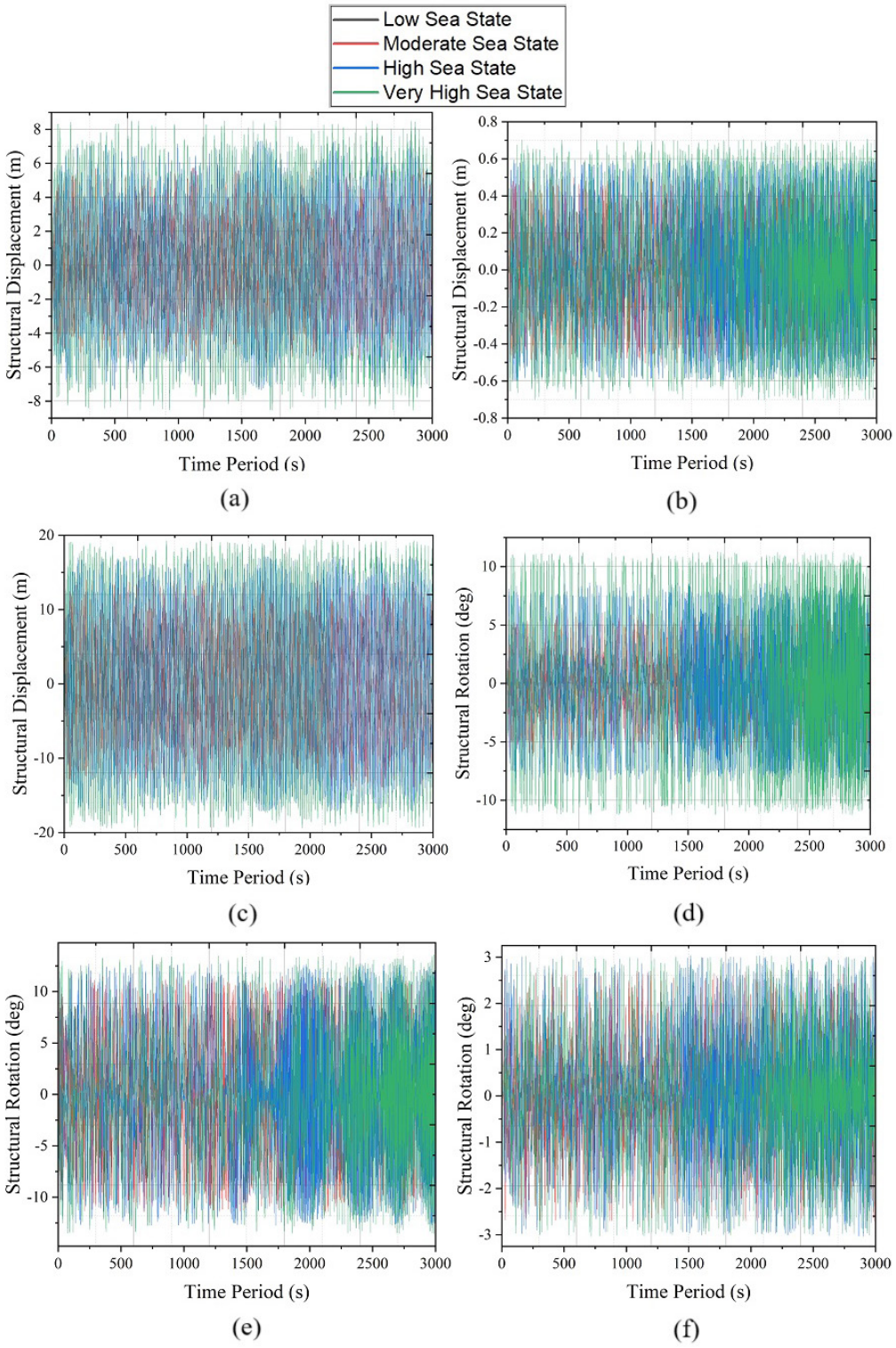

Figure 8 Responses in time domain for four distinct load cases; (a) Surge response, (b) Sway response, (c) Heave response, (d) Roll response, (e) Pitch response, (f)Yaw response.

The waves, wind, and currents responses have been compared under four distinct return periods. The response statistics are listed in **Table 9** above. The responses to an increase in sea roughness are reflected in all DOFs, which is anticipated by the rise in SD in various sea conditions. The response has a periodic pattern and varies in relation to the mean position. Compared to the low sea state, the RMS value increases in response to a surge of 2.464 and 3.063 times, respectively, in the high and very high sea states. In contrast to low sea states, the roll response RMS value rises in

very high and high sea states by 2.757 and 3.908 times, independently. The mean value declines as the RMS value increases in entire response levels, ranging from moderate to very high sea states. High and very high sea states of yaw response have maximum values of 1.548 and 1.594 times more significant than low sea states, respectively. Maximum peaks occur at the very high sea state responses for all the responses. Therefore, a very high sea state scenario was used for all the incident angle analyses.

Table 10 lists the very high sea state drillship dynamic responses under 0° to 180° wave heading incident angles. The drillship's dynamic behavior in various environmental scenarios and all wave heading angles is presented.

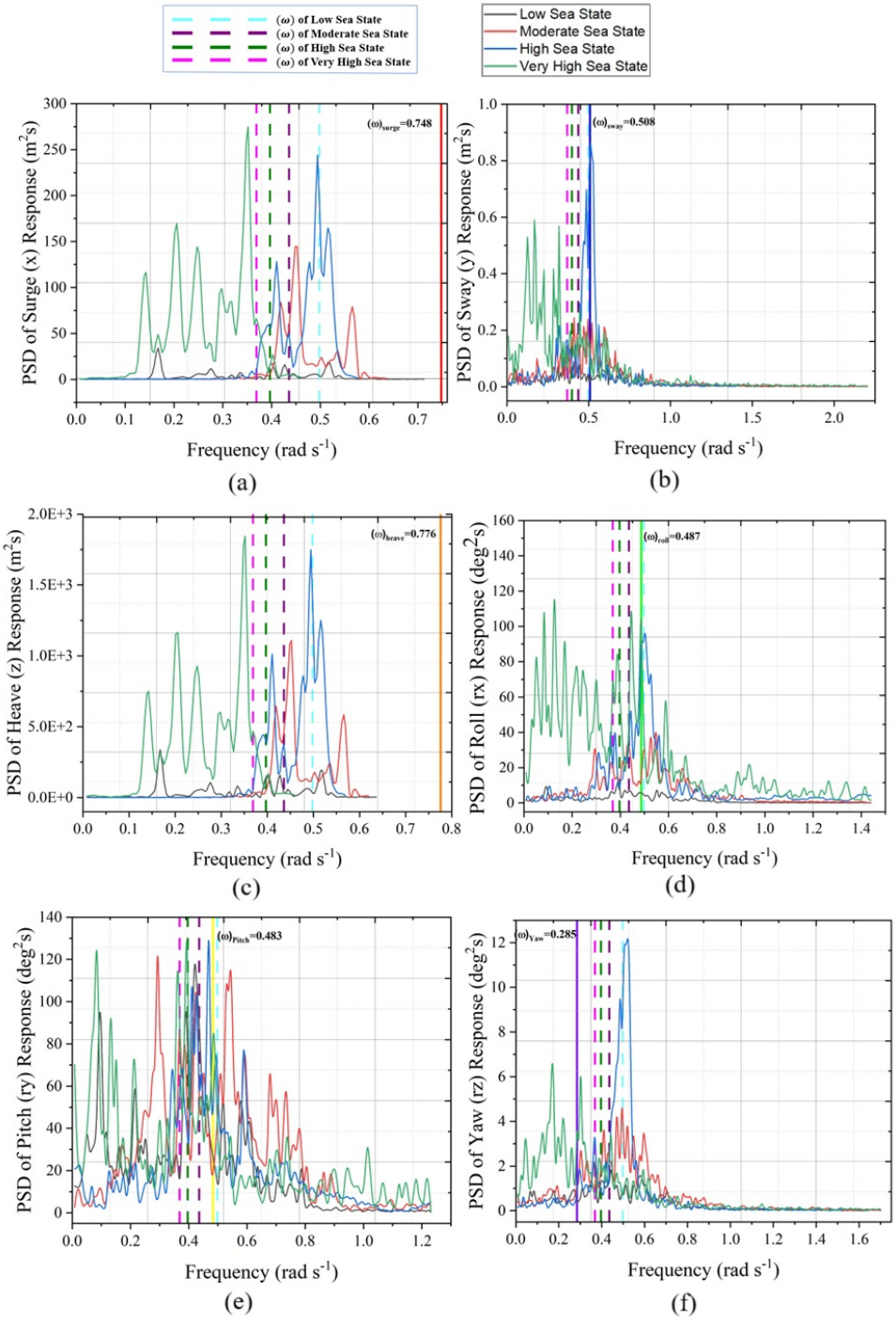

Figure 9 PSD responses under different sea states; (a) Surge response, (b) Sway response, (c) Heave response, (d) Roll response, (e) Pitch response, (f)Yaw response.

Table 9 Drillship structural response under various Hurricane Sea states at 180 deg heading incident angle.

Characteristics of Sea states	Descriptive Statistics	Surge response (m)	Sway response (m)	Heave response (m)	Roll response (deg)	Pitch response (deg)	Yaw response (deg)
Low sea state	Mean	0.02924	0.00191	0.15661	0.00480	-0.00655	0.02952
	SD	1.54618	0.17783	4.75566	1.63900	5.04780	0.79298
	Minimum	-3.61157	-0.38739	-10.01955	-3.40578	-8.81689	-1.92940
	Median	0.00085	0.00365	0.25963	0.01169	-0.03948	0.01441
	Maximum	3.62967	0.38752	9.98686	3.41284	8.81603	1.92719
	RMS	1.54643	0.17784	4.75816	1.63898	5.04754	0.79352
Moderate sea state	Mean	0.03353	-0.00731	0.08775	-0.11172	-0.05572	-0.03938
	SD	2.86249	0.26642	7.82836	3.18177	5.93618	1.11982
	Minimum	-5.73862	-0.50284	-14.08041	-6.12257	-11.52831	-2.70855
	Median	0.00887	-0.00531	0.16504	-0.05943	-0.03502	-0.02657
	Maximum	5.75350	0.50295	14.04907	6.13130	11.52812	2.70697
	RMS	2.86264	0.26651	7.82858	3.18365	5.93628	1.12042
High sea state	Mean	-0.01165	0.00514	0.10783	-0.02914	-0.09156	-0.00724
	SD	3.81057	0.32886	10.21595	4.52022	6.43597	1.22869
	Minimum	-7.33961	-0.59745	-17.16421	-8.61493	-12.73056	-3.03883
	Median	-0.00339	0.00233	0.15035	-0.01082	-0.16086	-0.00215
	Maximum	7.34937	0.59743	17.17394	8.62275	12.72982	3.03244
	RMS	3.81053	0.32889	10.21634	4.52024	6.43615	1.22869
Very high sea state	Mean	0.00025	0.00446	0.48475	-0.09801	-0.26497	-0.00833
	SD	4.73703	0.37544	12.17910	6.40625	6.45601	1.26409
	Minimum	-8.54742	-0.70355	-19.42178	-11.26697	-13.56134	-3.03807
	Median	0.018	0.00086	0.89712	-0.04811	-0.36799	-0.00013
	Maximum	8.50921	0.70686	19.41026	11.29336	13.60362	3.02807
	RMS	4.73695	0.37546	12.18840	6.40688	6.46101	1.26410

Table 10 Very high sea state drillship dynamic responses under various wave heading incident angles.

Incident Approach Angle	Analysis Statistics	Surge response	Sway response	Heave response	Roll response	Pitch response	Yaw response
0° Direction	Mean	0.01255	0.01745	0.12921	0.05580	-0.33180	0.02601
	SD	4.71866	0.36787	12.15014	6.30417	6.61854	1.28519
	Minimum	-8.53980	-0.70776	-19.43085	-11.28553	-13.60286	-3.03534
	Median	-0.02150	0.01335	0.35782	0.09961	-0.30666	0.00086
	Maximum	8.53085	0.70759	19.43473	11.27158	13.57609	3.01664
	RMS	4.71859	0.36828	12.15026	6.30424	6.62684	1.28541
30° Direction	Mean	0.01682	-0.01399	0.36766	-0.18671	-0.04594	0.02402
	SD	4.06438	2.37874	12.04740	6.28392	6.63687	1.25304
	Minimum	-7.39078	-4.30601	-19.39597	-11.26952	-13.58984	-3.03454
	Median	0.02339	0.01653	0.67364	-0.10617	-0.06024	0.02693
	Maximum	7.40954	4.30814	19.41001	11.28818	13.57123	3.03421
	RMS	4.06419	2.37862	12.05275	6.28637	6.63700	1.25326
60° Direction	Mean	-0.04922	-0.02476	0.35142	0.33074	0.98446	-0.09473
	SD	2.30740	4.02021	12.09434	6.07939	6.82749	1.25991
	Minimum	-4.30808	-7.41284	-19.42719	-11.29805	-13.54685	-3.03549
	Median	-0.01008	-0.00642	0.57499	0.11491	0.82699	-0.09256
	Maximum	4.30641	7.38491	19.4347	11.27286	13.58646	3.03091
	RMS	2.30787	4.02019	12.09883	6.08827	6.89809	1.26343
90° Direction	Mean	0.00214	0.02934	0.83283	-0.27575	0.33049	0.01565
	SD	0.37558	4.71908	12.12215	6.22910	6.52979	1.24575
	Minimum	-0.70723	-8.54377	-19.43263	-11.28915	-13.60721	-3.03531
	Median	0.00062	0.06863	1.48908	-0.14197	0.21772	0.02584
	Maximum	0.70763	8.54826	19.4355	11.25435	13.59359	3.02335
	RMS	0.37557	4.71904	12.15028	6.23507	6.53807	1.24576
120° Direction	Mean	0.01781	-0.00697	0.18003	0.23825	-0.36569	0.02816
	SD	2.33098	4.04015	12.07577	6.16063	6.78806	1.25578
	Minimum	-4.30729	-7.41316	-19.43359	-11.29578	-13.61051	-3.03700
	Median	-0.00233	0.01113	0.24214	0.13385	-0.35242	0.0069
	Maximum	4.30712	7.40882	19.40260	11.28658	13.59627	3.03309
	RMS	2.33089	4.03993	12.07682	6.16491	6.79789	1.25608
150° Direction	Mean	-0.00651	0.00892	0.12102	0.03738	-0.23538	-0.03039
	SD	4.00286	2.34025	12.00066	6.05416	6.89240	1.24106
	Minimum	-7.39408	-4.30816	-19.42323	-11.25747	-13.58904	-3.03344
	Median	0.01328	-0.00967	0.17620	0.10586	-0.16693	-0.01369
	Maximum	7.41175	4.30822	19.42115	11.29187	13.60117	3.03344
	RMS	4.00274	2.34020	12.00071	6.05415	6.89641	1.24141

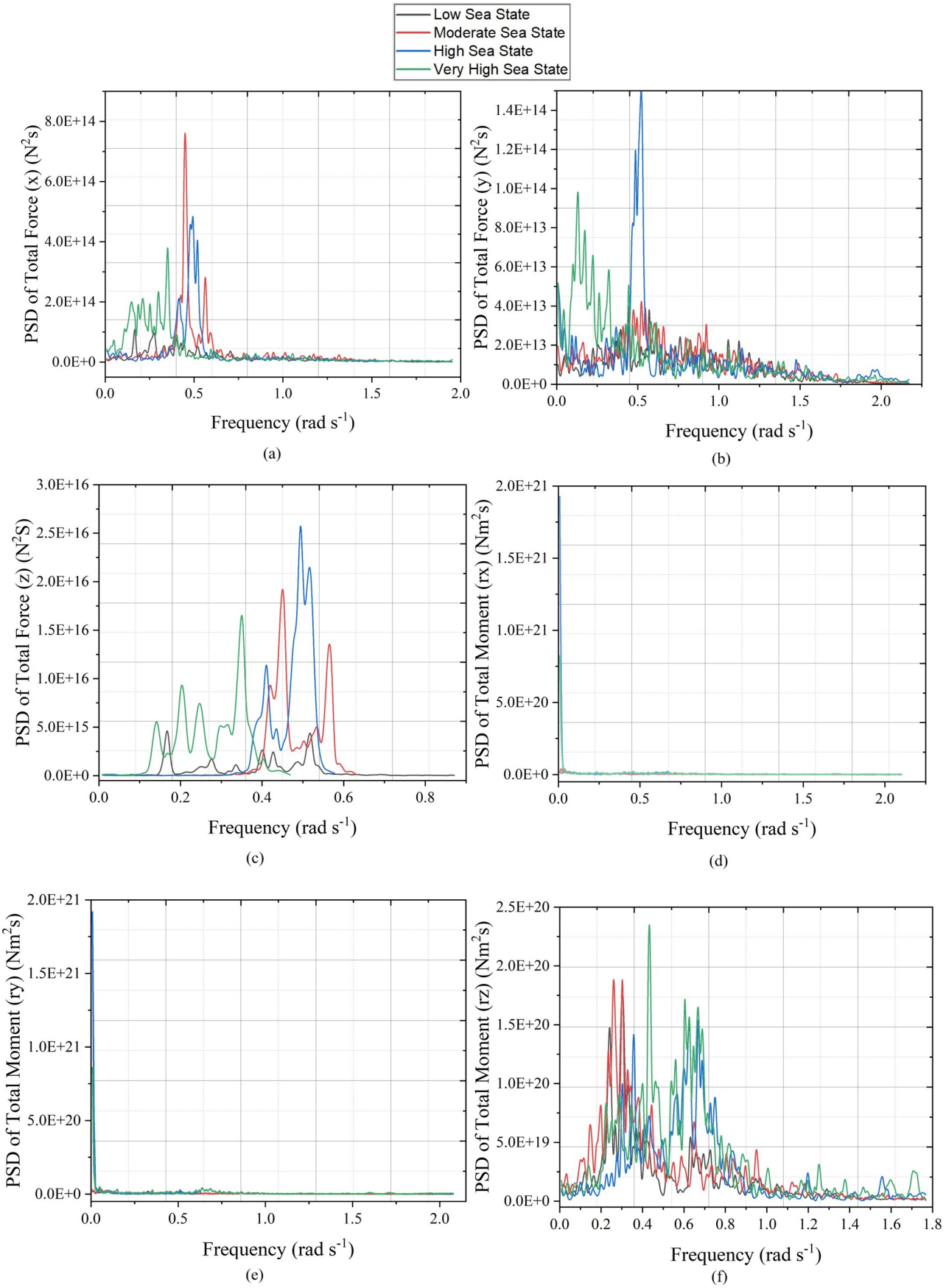

Figure 10 Total force/moment under different sea states; (a) Surge response, (b) Sway response, (c) Heave response, (d) Roll response, (e) Pitch response, (f)Yaw response.

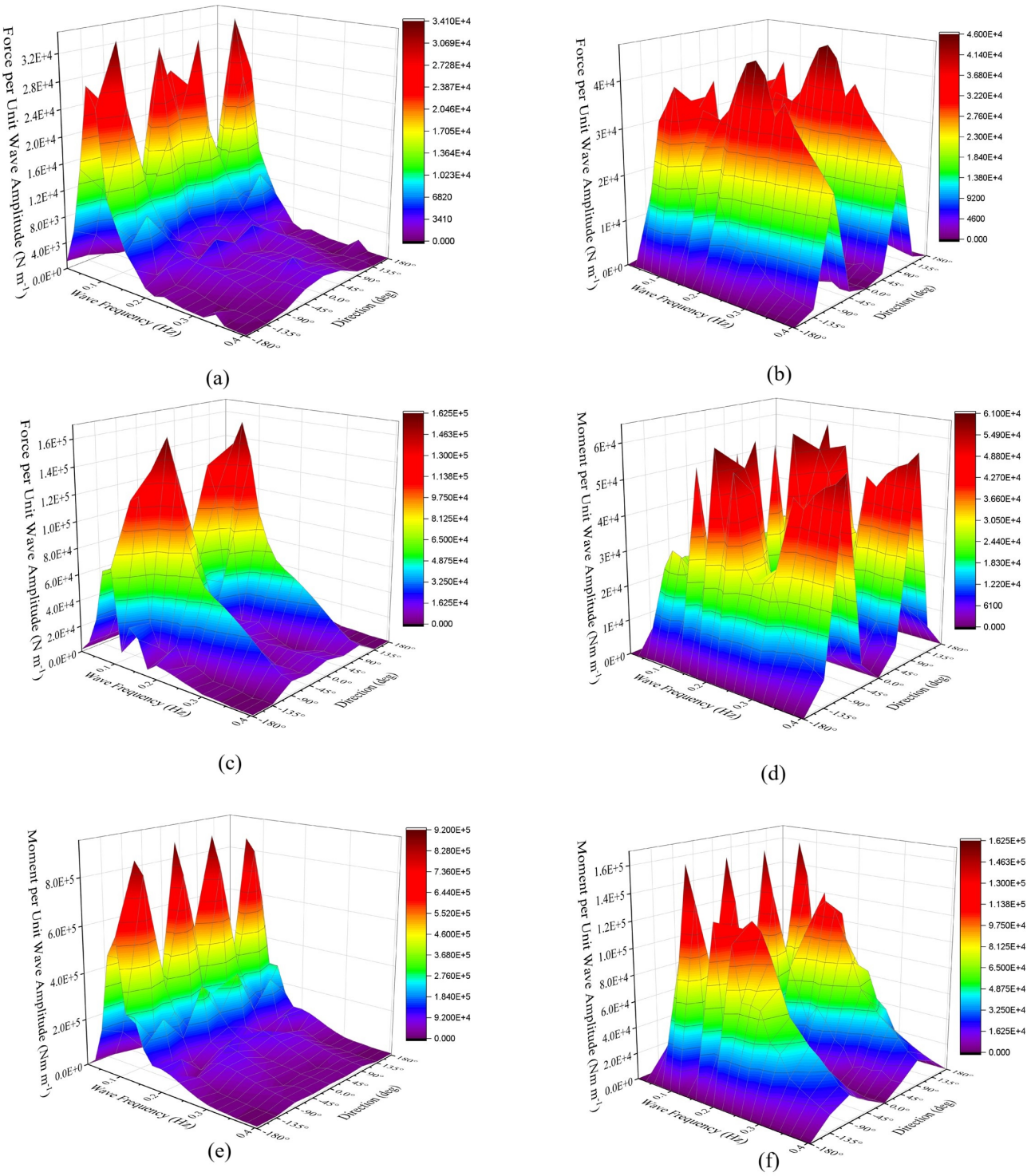

Figure 11 Shear force/bending moment (RAO); (a) Surge response, (b) Sway response, (c) Heave response, (d) Roll response, (e) Pitch response, (f) Yaw response.

4.2.3 Hydrodynamic total force/moment response analysis

Figure 10 shows the overall force and moment developed across all DOF under various sea states. As can be seen, Yaw motion imposes critical load conditions, as evidenced by the large moments acting about the vertical axis. These loads are particularly concerning, due to the high rotational stress they impose on the drillship's hull, leading to potential structural damage over time.

Prolonged exposure to yaw-induced forces, especially in critical environmental loads in the hull, causes excessive stress, resulting in fracking and panting. Therefore, a longitudinal/transverse shear will develop on the bottom hull, causing cracking. Further, roll and pitch moments dominate the condemnatory stresses in the rectangular moonpool region. The force amplitude per unit wave amplitude, as plotted in **Figure 11**, helps understanding of the influence of different sea states on the critical forces developed on the hull.

The conventional static wave technique calculates the design shear, as well as longitudinal bending moment after accounting for the coupled effect of pitch and heave motion. The combined impact of environmental loads and water level variances in the moonpool have amplified curvature due to longitudinal bending and shear. This combination has led to the development of critical stress levels in the structure of the moonpool, which has implications for its integrity and operational safety. Due to the higher magnitude of the added mass, the structural responses and the pressure on the hull increased for critical sea states. As seen, the pressure distribution around the hull and along the length varies, with higher pressures typically present near the waterline; it causes critical stress in the moonpool region.

5. Conclusions

The current work examines the hydrodynamic regular waves test, resistance properties, diffraction, Froude-Krylov, and impact analysis due to the ice loads of a drillship for an ultra-deep-sea environment. The drillship's time response during operational and survival wave circumstances provides essential information regarding the motion responses. The numerical calculations show that the drillship is relatively unstable, experiencing excessive roll and pitch, even during more extended periods of downtime. The moonpool shows a high-stress concentration. It is also seen that pitch response influences the design of shear and longitudinal bending. The moderate sea state imposes a significant roll and yaw response due to current and wave-coupled effects; surge motion reaches its maximum under very-high sea state circumstances. The roll motion changes based on whether the bottommost keel segment gets damaged and flooded during the bilging conditions. The drillship exhibits improved motion at deep abyssal water depths for the 10-year and 100-year return periods, as seen by the reduction in the roll response peak values. This enables safe operation in the pelagic field, along with a spread-mooring mechanism to control the response up to 1,000 m of sea depth. The investigation helps operators recognize regions where the drilling vessel’s efficiency can be enhanced, while minimizing the risk of mishaps or damage to the drillship.

Acknowledgments

The authors thank the support provided by the Indian Institute of Technology Madras, India, for the research assistance extended to carry out this study.

References

American Bureau of Shipping. (2011). *Drillship: Hull structural design and analysis*. American Bureau of Shipping, USA.

American Petroleum Institute. (2007). *API 2INT-MET: Interim Guidance on Hurricane Conditions in the Gulf of Mexico* (pp. 1-54). API Recommended Practice, USA.

Bharti, R., Pranesh, B., Sathianarayanan, D., Palaniappan, M., & Ramadass, G. A. (2024). Added mass analysis of submersible using computational fluid dynamics. *Maritime Technology and Research*, *6*(2), 267954. https://doi.org/10.33175/mtr.2024.267954.

Chandrasekaran, S. (2020). *Offshore semi-submersible platform engineering* (pp. 1-240). CRC Press, Florida. https://doi.org/10.1201/9781003130925

Chandrasekaran, S., & Chinu, P. (2024). Dynamic analysis of offshore triceratops supporting wind turbine: Preliminary studies. *Maritime Technology and Research*, *6*(1), 265564. https://doi.org/10.33175/mtr.2024.265564

Chandrasekaran, S., & Jain, A. (2017). *Ocean structures: Construction, materials and operations*. CRC Press, Florida. https://doi.org/10.1201/9781315366692

Chandrasekaran, S., & Nagavinothini, R. (2020). *Offshore compliant platforms: Analysis, design, and experimental studies*. John Wiley & Sons.

Chandrasekaran, S., & Selvakumar N. M. (2023). *Dynamic analysis of drillship under critical environmental loads* (pp. 2366-2373). In Proceedings of the International Ocean and Polar Engineering Conference. ISOPE-I-23-342.

Chandrasekaran, S., Sharma, R., & Selvakumar, N. M. (2023). Dynamic analysis of drillship under extreme metocean hurricane condition in ultra-deep water. *Journal of Marine Science and Technology*, *28*(4), 784-803. https://doi.org/10.1007/s00773-023-00957-2

Chandrasekaran, S., & Srivastava, G. (2018). *Design aids of offshore structures under special environmental loads including fire resistance* (Vol. 11). Singapore: Springer.

Choi, S. Y., Lee, Y. G., Jeong, K. L., & Ha, Y. J. (2011). Reduction of added resistance by internal flow control in the moonpool of a drillship. *Journal of the Society of Naval Architects of Korea*, *48*(6), 544-551. https://doi.org/10.3744/snak.2011.48.6.544

do Vale Machado, L., & Fernandes, A. C. (2022). Moonpool dimensions and position optimization with Genetic Algorithm of a drillship in random seas. *Ocean Engineering*, *247*, 110561. https://doi.org/10.1016/j.oceaneng.2022.110561

DNV, R. (2011). *H103 Modelling and Analysis of Marine Operations*. Høvik, Norway: Det Norske Veritas.

DNV. (2021). *Structural design of offshore ships, DNV- OS - C102, OSLO*. Norway: Det Norske Veritas.

DNV-RP-F205. (2010). *Global performance analysis of deepwater floating structures*. Oslo, Norway: Det Norske Veritas.

IMO. (2008). *Adoption of the International Code on Intact Stability.* IMO publications, London, UK.

ITTC. (2021). *Report of the seakeeping committee*. In Proceedings of the 29th International Towing Tank Conference, Switzerland.

Kaewkhiaw, P. (2025). Application of CFD to analyze the propeller guard kits' impact on hydrodynamic performance for Long-Tail Boat propellers in Thailand. *Maritime Technology and Research*, *7*(2), 272425. https://doi.org/10.33175/mtr.2025.272425

Korde, U. A. (1998). Active heave compensation on drill-ships in irregular waves. *Ocean Engineering*, *25*(7), 541-561. https://doi.org/10.1016/s0029-8018(97)00028-0

Lee, H. W., & Roh, M. I. (2018). Review of the multibody dynamics in the applications of ships and offshore structures. *Ocean Engineering*, *167*, 65-76. https://doi.org/10.1016/j.oceaneng.2018.08.022

Liu, Z., He, J., Meng, Y., Zhang, H., Zhou, Y., & Tao, L. (2022). Numerical and experimental study on the influence of a moonpool on motion performance and stability of a drillship. *Ocean Engineering*, *262*, 112241. https://doi.org/10.1016/j.oceaneng.2022.112241

Mauro, F., Della Valentina, E., Ferrari, V., & Begovic, E. (2023). A method for early-stage design current loads determination on drill-ships. *Ocean Engineering*, *287*, 115716. https://doi.org/10.1016/j.oceaneng.2023.115716

Molin, B. (2001). On the piston and sloshing modes in moonpools. *Journal of Fluid Mechanics*, *430*, 27-50. https://doi.org/10.1017/s0022112000002871

Norwood, M. N., & Dow, R. S. (2013). Dynamic analysis of ship structures. *Ships and Offshore Structures*, *8*(3-4), 270-288. https://doi.org/10.1080/17445302.2012.755285

Olapoju, O. M. (2023). Autonomous ships, port operations, and the challenges of African ports. *Maritime Technology and Research*, *5*(1), 260194. https://doi.org/10.33175/mtr.2023.260194

Rawson, K. J., & Tupper, E. C. (2001). *Basic Ship Theory- Vol. 1, Butterworth-Heinemann*. Oxford, UK. https://doi.org/10.1016/b978-075065398-5/50018-2

Saengsupavanich, C., Coowanitwong, N., Gallardo, W. G., & Lertsuchatavanich, C. (2009). Environmental performance evaluation of an industrial port and estate: ISO14001, port state control-derived indicators. *Journal of Cleaner Production*, *17*(2), 154-161. https://doi.org/10.1016/j.jclepro.2008.04.001

Sharma, R., Kim, T. W., Sha, O. P., & Misra, S. C. (2010). Issues in offshore platform research-Part 1: Semi-submersibles. *International Journal of Naval Architecture and Ocean Engineering*, *2*(3), 155-170. https://doi.org/10.2478/ijnaoe-2013-0032

Srinivasan, C., & Nagavinothini, R. (2019). Ice-induced response of offshore triceratops. *Ocean Engineering*, *180*, 71-96. https://doi.org/10.1016/j.oceaneng.2019.03.063

Srinivasan, C., Shah, B., & Chauhan, Y. J. (2022). Dynamic analyses of triceratops under Hurricane-driven Metocean conditions in Gulf of Mexico. *Ocean Engineering*, *256*, 111511. https://doi.org/10.1016/j.oceaneng.2022.111511

Suja, T. P., & Chandrasekaran, S. (2025). Response control of TLP with Single TMD under wind, wave, and current: TLP with TMD. *Maritime Technology and Research*, *7*(1), 272515. https://doi.org/10.33175/mtr.2025.272515

Tikhonov, V. S., Komissarenko, V. I., & Emec, B. V. (1991). Dynamic behaviour of deepwater drilling column under collisions with drillship moonpool. *Applied Ocean Research*, *13*(6), 307-316. https://doi.org/10.1016/s0141-1187(05)80054-9

Wang, H., Meng, X., & Chen, C. (2022). Cross-correlation analysis of wind speeds and displacements of a long-span bridge with GNSS under extreme wind conditions. *Maritime Technology and Research*, *4*(3), 254407. https://doi.org/10.33175/mtr.2022.254407

Yang, S. H., Lee, S. B., Park, J. H., Han, S. Y., Choi, Y. M., Do, J., Kwon, S. H., & Molin, B. (2016). Experimental study on piston-and sloshing-mode moonpool resonances. *Journal of Marine Science and Technology*, *21*, 715-728. https://doi.org/10.1007/s00773-016-0386-x

Yu, S., Wang, L., Li, B., & He, H. (2020). Optimal setpoint learning of a thruster-assisted position mooring system using a deep deterministic policy gradient approach. *Journal of Marine Science and Technology*, *25*, 757-768. https://doi.org/10.1007/s00773-019-00678-5

Yuda, I. D. G., Djatmiko, E. B., & Rosyid, D. M. (2015). A study of the dynamic longitudinal hull structural responses and ultimate strength of drillship. *Science and Engineering*, *17*, 1-8. http://dx.doi.org/10.13140/RG.2.1.4770.9208